

DETC97/VIB-3929

IMPACT DYNAMICS OF A SUPERCAVITATING UNDERWATER PROJECTILE

Richard Rand
Cornell University
Ithaca, NY 14853

Rudra Pratap
Indian Institute of Science
Bangalore, India

Deepak Ramani
Cornell University
Ithaca, NY 14853

Jeffery Cipolla
Naval Underwater Weapons Center
Newport, RI 02841

Ivan Kirschner
Naval Underwater Weapons Center
Newport, RI 02841

ABSTRACT

We investigate the in-flight dynamics of a simplified model of a supercavitating body. In particular we are interested in the nature and frequency of the impacts which occur as the tail of the body touches the cavity walls. Referring to laboratory experiments conducted at Cal Tech in the 1950's, we show that the tip force by the fluid is approximately directed along the length of the body. This gives zero moment about the body's center of mass which leads us to assume that the body moves as if it were a moment-free rigid body pinned at its tip. To simplify the analysis, we assume that the body is not spinning about its symmetry axis. Then the motion between impacts is a plane motion with constant angular velocity. Using elementary fluid mechanics, we model the impact occurring when the tail touches the cavity walls, and we show that it is reasonable to assume that the impact is instantaneous with coefficient of restitution unity. Using this simplified model, we offer a simulation for typical parameters.

INTRODUCTION

Underwater vehicles such as torpedoes and submarines are limited in maximum speed by the considerable drag produced by the flow friction on the hull skin. Speeds of 40 m/s (75 knots) are considered very high; most practical systems are limited to less than half this figure. While low speed is advantageous for acoustics and hydrodynamic efficiency, some special applications requiring high speed cannot be realized using conventional hydrodynamics. When a body

moves through water at sufficient speed, the fluid pressure may drop locally below a level which sustains the liquid phase, and a low-density gaseous 'cavity' can form. Flows exhibiting cavities enveloping a moving body entirely are called 'supercavitating', and, since the liquid phase does not contact the moving body through most of its length, skin drag is almost negligible.

Several new and projected underwater vehicles exploit supercavitation as a means to achieve extremely high submerged speeds and low drag (Miller, 1995). The sizes of existing or notional supercavitating high-speed bodies range from that of bullets (for example the Adaptable High-Speed Undersea Munition, AHSUM, or the projectiles of the Rapid Airborne Mine Clearance System, RAMICS) to that of full-scale heavyweight torpedoes. Since the forces on a supercavitating body are so different from those on conventional submerged bodies, hydrodynamic stability issues need to be completely reassessed. In particular, since the body is wetted only for a tiny percentage of its length, and since vapor dynamic forces are nearly negligible, the center of pressure will nearly always be ahead of the center of mass, violating a standard principle of hydrodynamic stability. Also, the body dynamics consist of at least two qualitatively different phases: pure supercavitating flight, with only tip contact with the fluid, and states including contacts with the fluid cavity walls. See Fig.1.

In the case of pure supercavitating flight, forces produced by the flow of water vapor may be a significant sta-

bilizing effect at very high speeds. In the case that the body touches the cavity walls, these contacts may be of long-duration (planing), or intermittent (impacts). In this initial study, we consider intermediate speed regimes where long-duration cavity contact (planing) does not occur, and where vapor dynamic forces are negligible.

In this paper we investigate the in-flight dynamics of a simplified model of a supercavitating body. In particular we are interested in the nature and frequency of the impacts which occur as the tail of the body touches the cavity walls.

MODELING ASSUMPTIONS

Our model is based on the following assumptions:

1. The path of the center of mass of the body is assumed to be well-approximated by a straight horizontal line L . This assumption neglects gravity, which is justified by experimental work which showed no effect of gravity at speeds greater than 8 m/sec ((May, 1975), p.2-28).

2. The cavity is assumed to be approximately fixed in an orientation which remains symmetric about the horizontal line L . This assumption represents a simplified model of the real motion of the cavity which traces a serpentine form as the body oscillates about the line of travel. The shape of the cavity is assumed to be a known function of the forward velocity of the body, although the only place this is used is in determining when the tail of the body touches the cavity walls, a condition referred to as 'tailslap'. The diameter of the cavity, and hence the clearance between the tail and the cavity walls, is known to decrease as forward velocity decreases. This clearance is small compared to the length of the body, permitting the assumption that the body axis B always makes a small angle θ with the cavity axis L .

3. The projectile is assumed to rotate about the nose tip. In fact, the center of rotation in a quasi-inertial coordinate system translating with the body will not in general be at the nose. However, if the wavelength of the disturbances in the fluid caused by tailslap is much greater than the projectile length, then the geometry of tailslap dynamics can be well approximated by assuming that the shape of the translating cavity is frozen and the center of rotation is at the nose. This was the case in previous AHSUM tests, where the tailslap frequency was on the order of 600 Hz when the projectile speed was approximately 600 m/s.

4. In the absence of impacts, we assume that the only force on the body is due to the fluid force at the tip. Laboratory experiments (May, 1975), (Kiceniuk, 1954) have shown that the net tip force acts approximately along the axis of the body B with zero net applied moment. See Appendix

A. The magnitude F of the tip force is:

$$F = \frac{1}{2} \rho A v^2 k \cos \theta \quad (1)$$

where ρ = density of water,

A = cross-sectional area of the tip,

$v = \dot{x}$ = forward velocity,

k = a nondimensional constant,

θ = angle between the body axis B and the cavity axis L .

5. We model the impact of the tail against the cavity walls (tailslap) as occurring instantaneously with coefficient of restitution of unity. Appendix B contains an analysis of this problem from which we conclude that the duration of a single impact is on the order of 10^{-4} sec to 10^{-2} sec.

6. In order to simplify the analysis we assume that the body is not spinning about its symmetry axis B .

In view of the foregoing assumptions, the in-flight dynamics may be decomposed into a translatory motion and rotation of the body. The translatory motion is uninfluenced by the rotation of the body. The rotation of the body is influenced by the translatory motion because the size of the cavity is dependent on the forward velocity, and this influences the period of time between impacts.

FORWARD MOTION

In order to determine the translatory motion of the body, let x measure the horizontal distance of the center of mass from a fixed datum, say the launch site. The motion in the x -direction is impeded by the drag force at the tip F_D . This neglects the effect of the impact forces, which for small angles of tilt θ are nearly perpendicular to the horizontal line L . See Fig.2.

Carrying out $\sum F = ma$ in the x -direction, we get (see Appendix A):

$$m\ddot{x} = -F_D = -\frac{1}{2} \rho A \dot{x}^2 k \cos^2 \theta \quad (2)$$

For small values of θ this becomes:

$$\ddot{x} = -\alpha \dot{x}^2 \quad (3)$$

where $\alpha = \frac{\rho A k}{2m}$. Eq.(3) has the solution:

$$x(t) = \frac{1}{\alpha} \ln(1 + \alpha \dot{x}_0 t) \quad (4)$$

where \dot{x}_0 is the body's initial velocity. The velocity $\dot{x}(t)$ is given by:

$$\dot{x}(t) = \frac{\dot{x}_0}{1 + \alpha \dot{x}_0 t} \quad (5)$$

ROTATORY MOTION

During the period of motion between successive impacts, the only force on the body is the tip force F which is directed along the body axis B . Thus the sum of the moments about the center of mass is zero, and the body moves as if it were a moment-free rigid body pinned at its tip. In view of assumption 6, that the body is not spinning about its symmetry axis, the motion between impacts is a plane motion with constant angular velocity. After each impact the plane of this motion will, in general, change, while the magnitude of its angular velocity will remain constant (by assumption 5 that the coefficient of restitution is unity).

In Fig.3 we view the body from behind, looking at a plane normal to the cavity symmetry axis L , taken at a section near the tail (Greenwood, 1988). Between impacts the tail will move across this plane in an approximately straight line with constant speed corresponding to a rotation of the body with constant angular velocity. This approximation is valid for small angles of deflection. At each impact, in view of assumption 5, the angle of incidence will equal the angle of reflection. Given an initial position and velocity of the tail, a series of impacts and reflections will occur. These will be influenced by the diameter of the cavity at this section, which becomes smaller as the forward speed of the body decreases, thereby increasing the frequency of impacts.

NUMERICAL RESULTS

In order to obtain sample simulated results, we assumed the following values of the parameters:

$$\begin{aligned} \rho &= 1000 \text{ kg/m}^3 \\ A &= \pi(0.001)^2 \text{ m}^2 \\ m &= 0.15 \text{ kg} \\ k &= 0.9 \\ l &= 0.12 \text{ m} \\ d &= 0.015 \text{ m} \\ \lambda &= 0.5 \\ a &= l/2 = 0.06 \text{ m} \\ I &= ml^2/12 = 0.00018 \text{ kg m}^2 \end{aligned}$$

In addition, we assumed a linear relation between h , the distance from the centerline L to the cavitation region boundary at the tail, and \dot{x} :

$$h(\dot{x}) = 2.857 \times 10^{-5} \dot{x} + 0.00714 \quad (6)$$

This relation is chosen so that $h = 0.05$ m when $\dot{x} = 1500$ m/sec and $h = 0.01$ m when $\dot{x} = 100$ m/sec.

For initial conditions, we chose $\dot{x}_0 = 1500$ m/sec and we took the body axis B to be initially inclined to the cavity axis L by an angle of 0.01 rad with an initial angular velocity of 1 rad/sec in a direction perpendicular to the plane determined by axes B and L . The resulting numerical results are displayed in Figs. 4 and 5.

In the case that the initial clearance between the projectile tail and the cavity is smaller (say about 3 mm) we find that the projectile tends to "roll" around the cavity walls via a series of rapidly occurring tailslaps.

DISCUSSION AND CONCLUSIONS

Our model predicts that as the projectile races through the water, it rotates like a moment-free rigid body about the point where its nose touches the water. For typical initial conditions, this leads to impacts of its tail with the cavity walls. These impacts become more frequent as the body slows down, since the diameter of the cavity decreases with a decrease in forward speed. The number of impacts achieved in a given time interval (e.g. in one second) depends on the initial conditions of the body. The larger the initial angular velocity, the greater the number of impacts. The dynamics are also found to depend on the initial deflection angle. Motions which are positioned so that they strike the cavity walls more nearly tangentially have a shorter distance to travel before their next impact, and so encounter more impacts in a given time interval.

These conclusions are based on the extremely simplified nature of the model. For example, we assumed that the projectile had no spin about its body axis B . Spin could result from rifling in the barrel of the launch device. If spin were included in the model, the resulting gyroscopic effects could, for some initial conditions, eliminate impacts. The general motion of a moment-free rigid body is well-known to involve precession without nutation (Greenwood, 1988). If the initial conditions started the spinning body close to the cavity symmetry axis L with an appropriate angular velocity, the body might avoid striking the cavity walls during a given time period. On the other hand, we have not yet investigated the impact dynamics for the case of the spinning body.

An extension of this work could include modeling the fluid reaction forces more accurately. In particular the assumption that the cavity remains fixed in orientation could

be replaced by a model in which the cavity rotates, following the rotatory motion of the body, but with a delay.

ACKNOWLEDGMENT

Research performed under the Naval Undersea Warfare Center Division, Newport, RI, Supercavitating High-Speed Bodies Program; I. Kirschner, Chief Engineer and Principal Investigator; C. Curtis, Program Manager. Research sponsored by the Office of Naval Research Undersea Weaponry Basic Research Program, J. Fein, Program Manager (Program Element 0601153N, Project No.BR02301).

REFERENCES

- D. Miller, "Supercavitation: Going to War in a Bubble", *International Defense Review*, 61-63, December, 1995.
- A. May, "Water Entry and Cavity-Running Behavior of Missiles", *Navsea Hydroballistics Advisory Committee Technical Report SEAHAC/TR 75-2*, 1975.
- T. Kiceniuk, "An Experimental Study of the Hydrodynamical Forces Acting on a Family of Cavity-Producing Conical Bodies of Revolution Inclined to the Flow", *Cal. Inst. Tech. Hydrodynamics Lab. Report No. E-12.17*, 1954.
- D. T. Greenwood, *Principles of Dynamics*, second ed., p.382, Prentice-Hall, 1988.

APPENDIX A: THE TIP FORCE

In the absence of impacts, the only force on the body is assumed to be the force by the fluid at the body's nose. Our modeling of this fluid force is based on experimental results quoted in (May, 1975), p.2-24, Fig.2-36, which are themselves based on Fig.6 in (Kiceniuk, 1954). To begin with, we neglect any applied moment at the nose. Further, we assume that the net force acts along the axis of the body. This key assumption is based on the estimates

$$C_D = k \cos^2 \theta \quad \text{and} \quad C_L = k \sin \theta \cos \theta \quad (7)$$

where the drag force F_D and the lift force F_L are given by

$$F_D = \frac{1}{2} \rho A v^2 C_D \quad \text{and} \quad F_L = \frac{1}{2} \rho A v^2 C_L \quad (8)$$

where ρ =density of water,
 A =cross-sectional area of the tip,
 $v = \dot{x}$ =forward velocity,

k =a nondimensional constant,

θ = angle between the body axis B and the cavity axis L .
 These estimates agree with (May, 1975), p.2-24, where we find that " C_D ... decreases approximately as $\cos^2 \alpha$ " and "For small angles of attack, the lift force ... is nearly equal to $\sin \alpha$ times the drag force at $\alpha = 0$ ", where $\alpha = \theta$ is the angle of attack. Thus $C_L/C_D = \tan \theta$ and the force by the fluid at the body's nose is directed along the body axis B . See Fig.6. Eq.(1) for the magnitude of the associated force F follows from eqs.(7),(8).

APPENDIX B: IMPACT MODEL

Here we discuss the tail forces encountered during impact of the body with the cavity walls. Let $\delta(t)$ represent the maximum penetration distance of the tail into the surrounding fluid, see Fig.7.

We see that

$$\delta = l \sin \theta + \frac{d}{2} \cos \theta - h \quad (9)$$

where l = length of body,

d = diameter of body at tail,

$h = h(\dot{x})$ = distance from line L to cavity walls at tail section.

In order to obtain an estimate for the fluid forces on the tail during impact, we perform a momentum transfer calculation based on the geometry in Fig.8.

Here a layer of fluid of thickness $\lambda \delta$ is deflected from its original course parallel to the direction of flight, line L , by the tail, through an angle θ . Momentum balance gives the force on the tail as:

$$R_D = \rho A_1 v^2 (1 - \cos \theta) \quad \text{and} \quad R_L = \rho A_1 v^2 \sin \theta \quad (10)$$

where R_D and R_L are components of the tail force, see Fig.9, and where

ρ = density of water,

$A_1 = \lambda \delta d$ = cross-sectional area of fluid layer,

$v = \dot{x}$ = forward velocity.

To simplify the following discussion, which is aimed at estimating the duration of a single impact, we restrict attention to the case in which the body strikes the cavity walls normally, i.e. in which the motion of the body is two dimensional. The tail forces R_D and R_L act at the center of pressure of the fluid forces on the tail, assumed to be close to the body axis B . Writing $\sum M = I \ddot{\theta}$ about the center of mass, we obtain (see Fig.9):

$$I \ddot{\theta} = -R_D a \sin \theta - R_L a \cos \theta \quad (11)$$

where I = transverse moment of inertia of the projectile about its center of mass, a = distance from the center of mass to point of application of the tail forces.

Using eq.(10) this becomes

$$I \ddot{\theta} = -\rho A_1 v^2 a \sin \theta \quad (12)$$

Substituting for A_1 and v , we obtain

$$I \ddot{\theta} + \rho \lambda \delta d a \dot{x}^2 \sin \theta = 0 \quad (13)$$

Using eq.(9) for δ and assuming small angles θ , this becomes:

$$I \ddot{\theta} + \rho \lambda \left[l \theta + \frac{d}{2} - h \right] d a \dot{x}^2 \theta = 0 \quad (14)$$

Eq.(14) is valid only so long as $\delta > 0$, i.e. so long as the tail contacts the cavity wall, i.e., $\theta > (2h - d)/(2l)$. Simplification results by replacing θ by ϕ , defined as:

$$\phi = \theta - \frac{2h - d}{2l} > 0 \quad (15)$$

Substituting eq.(15) into (14) and treating $h(\dot{x})$ like a constant (since the duration of the impact is small), we obtain for small ϕ :

$$\ddot{\phi} + \omega^2 \phi = 0 \quad (16)$$

where

$$\omega^2 = \frac{\rho \lambda d a}{I} \left[h - \frac{d}{2} \right] \dot{x}^2. \quad (17)$$

Eq.(16) holds from the time that ϕ becomes zero (tail entering the cavity wall) until it becomes zero again (tail exiting cavity wall). Thus the duration of the impact is half the period of the simple harmonic oscillator (16):

$$\text{impact duration} = \frac{\pi}{\omega} \quad (18)$$

Substituting the sample numerical values given in the body of the paper, we find that impact duration varies between 0.0002 sec to 0.012 sec as \dot{x} varies between 1500 m/sec to 100 m/sec. The absence of damping in eq.(16) implies that we have modeled the tailslap as involving no energy loss.

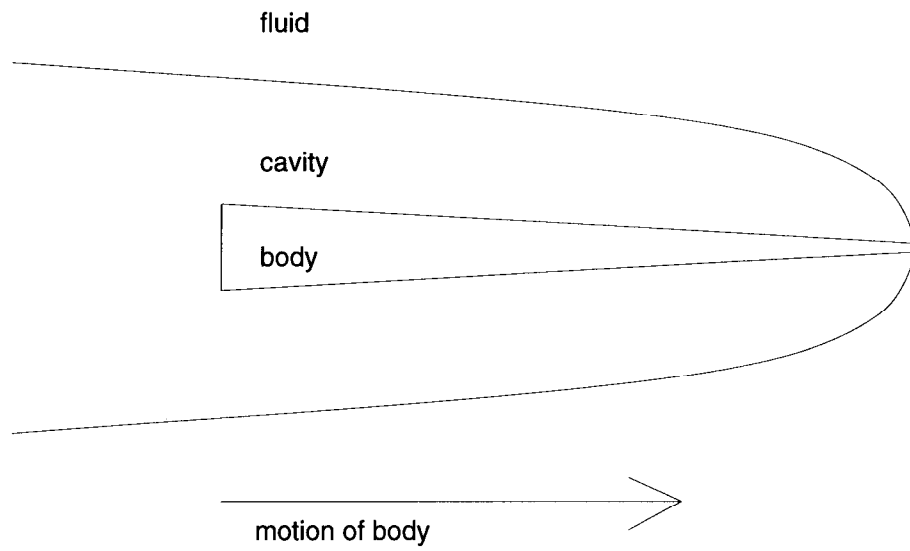


Fig.1. Supercavitating projectile.

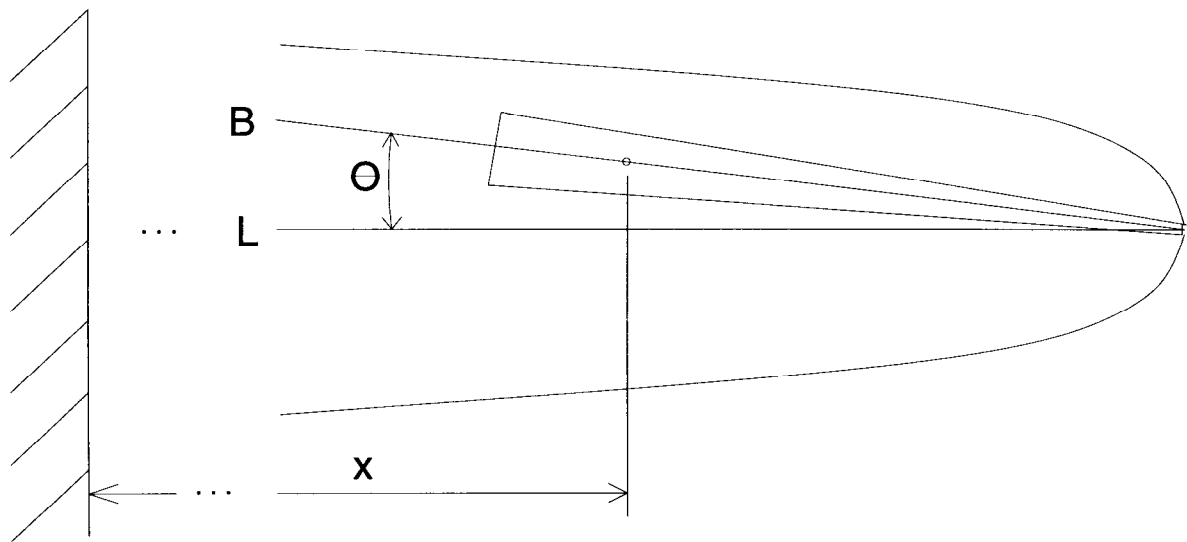


Fig.2. Supercavitating projectile showing coordinates x and θ . We are looking at the plane determined by the body axis B and the cavity symmetry axis L . This view omits a third coordinate which determines which meridional plane we are in.

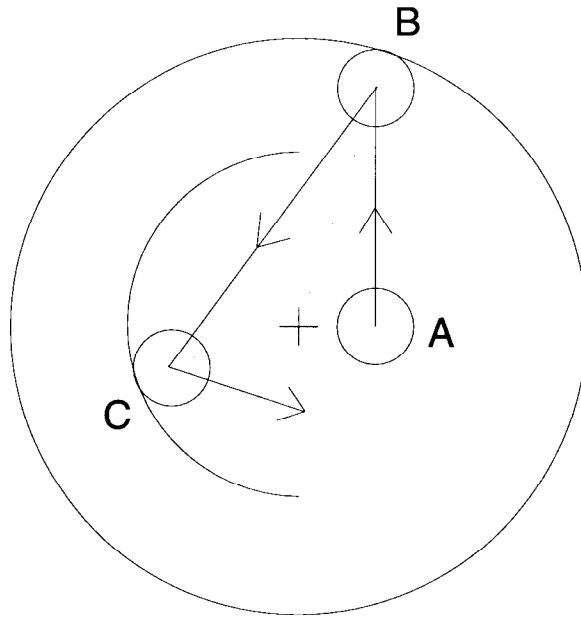


Fig.3. View of the body from behind. The '+' marks the line L , symmetry axis of the cavity. Tail in position A moves to B where it impacts against the cavity wall represented by the outer circle. After impact, tail moves from B to C where it again impacts against the cavity wall, the diameter of which has become smaller. The body rotates in a plane about the nose (which is not seen in this view from behind), resulting in the tail moving in a straight line in this view (an approximation valid for small deflection angles).

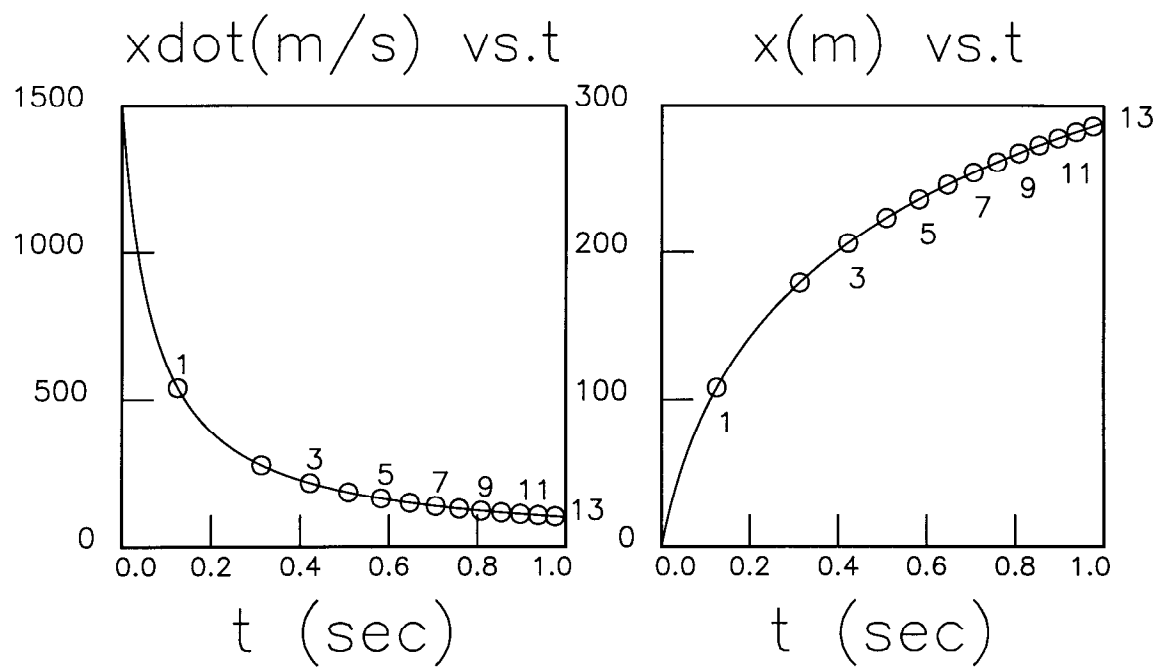


Fig.4. Forward motion from a sample simulation. The projectile, released with initial velocity 1500 m/sec, travels about 300 m in 1 sec, at which point its velocity is about 100 m/sec. The impacts between the tail of the body and the cavity walls are displayed as numbered circles, cf.Fig.5.

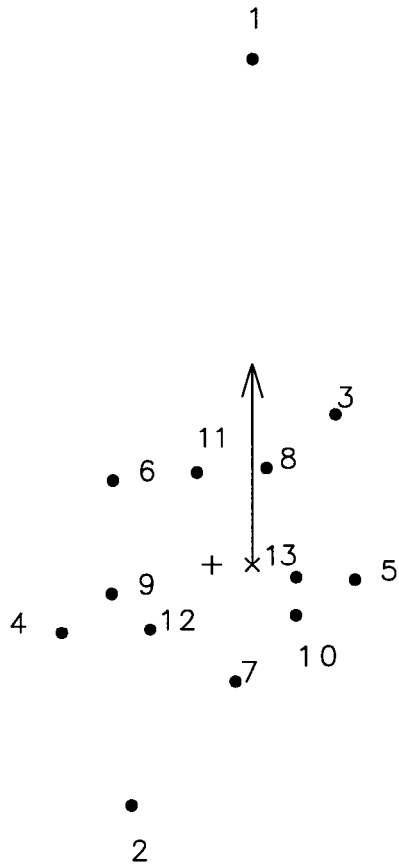


Fig.5. Successive impacts from a sample simulation. We see a view from behind the body. The '+' marks the line L , symmetry axis of the cavity. The 'x' marks the initial position of the tail. The arrow represents the initial angular velocity of the body, here shown as the corresponding linear velocity of the tail. Each dot represents the position of the body axis B during the first 13 impacts, all of which occurred in the first second of simulated flight. Each impact corresponds to a progressively smaller cavity size.

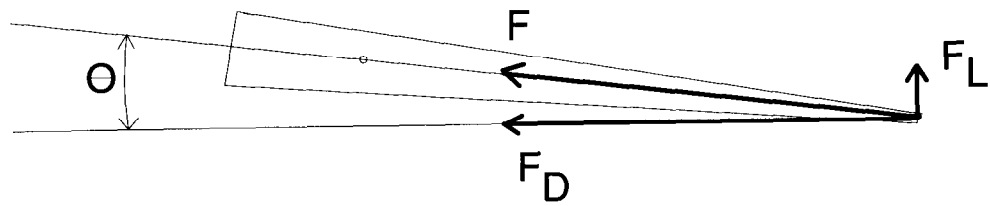


Fig.6. Fluid forces on the projectile's nose. F is the resultant of lift F_L and drag F_D forces.

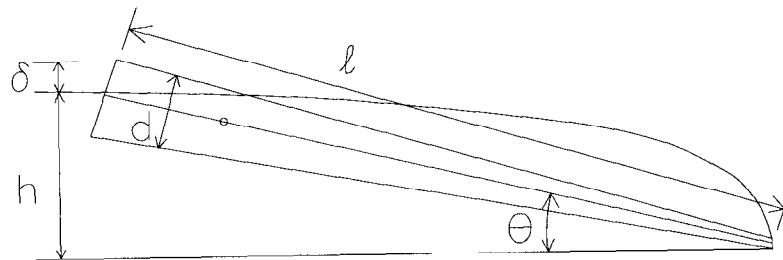


Fig.7. Geometry of impact: projectile tail enters the surrounding fluid.

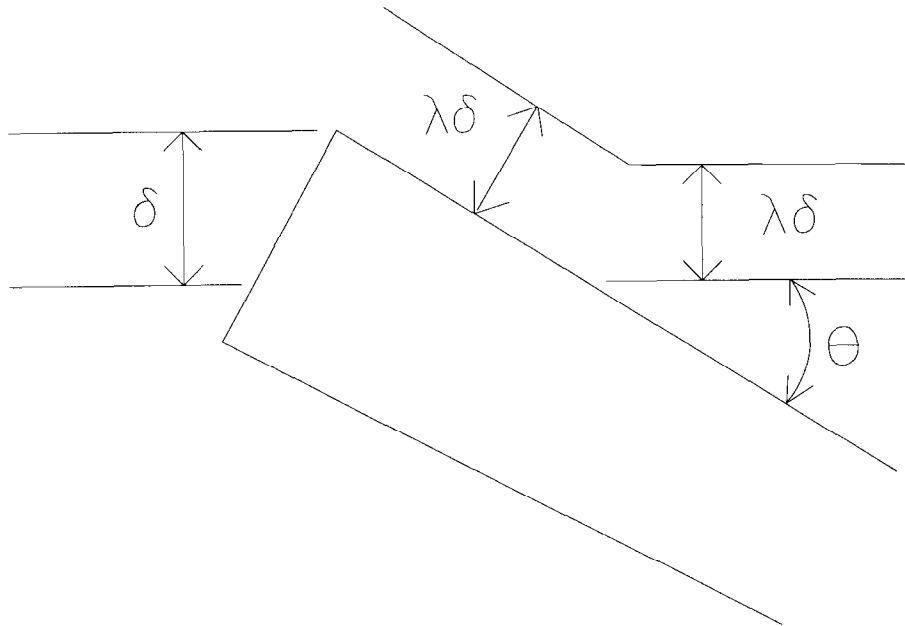


Fig.8. Momentum transfer calculation.

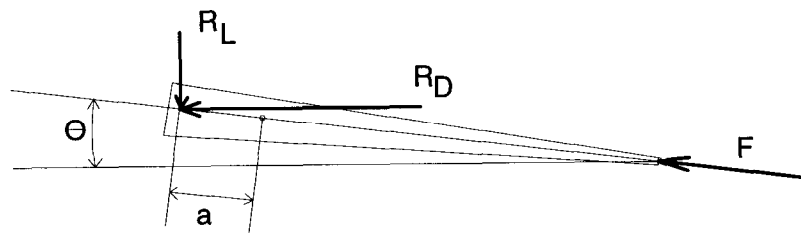


Fig.9. Free body of projectile during impact. Dot marks center of mass.